Digest Journal of Nanomaterials and Biostructures Vol. 7, No. 3, July - September 2012, p. 1343 - 1352

TiO_2/ZrO_2 THIN FILMS SYNTHESIZED BY PLD IN LOW PRESSURE N-, C- AND/OR O-CONTAINING GASES: STRUCTURAL, OPTICAL AND PHOTOCATALYTIC PROPERTIES

OKSANA LINNIK[a], IRINA PETRIK[a], NATALIA SMIRNOVA[a], VIKTOR KANDYBA[b], OLEKSANDR KORDUBAN[b], ANNA EREMENKO[a], GABRIEL SOCOL[c], NICOLAIE STEFAN[c], CARMEN RISTOSCU[c*], ION N. MIHAILESCU[c], CLAUDIU SUTAN[d], VIOREL MALINOVSCHI[d], VELJKO DJOKIC[e], DJORDJE JANAKOVIC[e]
[a]O. O. Chuiko Institute of Surface Chemistry, National Academy of Science of Ukraine, 17 General Naumov str., Kyiv, 03164, Ukraine
[b]G.V. Kurdyumov Institute of Metallophysics, National Academy of Sciences of Ukraine, Acad. Vernadsky blvd. 36, Kyiv, 03680, Ukraine
[c]National Institute for Lasers, Plasma and Radiation Physics, 409 Atomistilor street, Magurele, PO Box MG-54, RO-77125, Ilfov, Romania;
[d]University of Pitesti, Research Centre for Advanced Materials, Targul din Vale Street, No 1, 110040, Pitesti, Arges, Romania
[e]Faculty of Technology and Metallurgy, University of Belgrade, Karnegijeva 4, 11000 Belgrade, Serbia

Doped TiO_2/ZrO_2 films were obtained by Pulsed Laser Deposition method under different synthesis conditions. The onset of absorption spectra was red shifted for the films obtained in N_2 containing gas mixtures, while a broad absorption in visible was observed in the case of films deposited in CH_4 atmosphere. The presence of O-Ti-N bonds revealed by XPS corresponded to the highest photocatalytic performance. XPS spectra of the samples obtained in N_2/CH_4 gas mixtures evidenced a more effective incorporation of nitrogen in the structure due to oxygen deficiency. Nevertheless, no atomic carbon presence in the TiO_2/ZrO_2 structures has been detected.

(Received June 20, 2012; Accepted September 6, 2012)

Keywords: TiO_2/ZrO_2 thin films, N- and C-doping, photocatalytic activity, toxic Cr(VI) ions reduction

1. Introduction

Heterogeneous photocatalysis based on the interaction of semiconductor particles with light has focused an enormous attention in environmental and energy-storing research fields. Photocatalysis is applied for the destruction and redox transformations of highly toxic inorganic or organic compounds, as well as for hydrogen production and solar energy conversion to electricity [1-4]. We note that titanium dioxide is an inexpensive semiconductor material, non-toxic, resistant to photocorrosion which is possessing high oxidative power. However, TiO_2 absorbs only 4 % of ultraviolet light and it is inert in the whole visible range of the solar spectrum. The challenge was therefore to extend the sensitivity of TiO_2 towards the visible range of the spectrum. One well-known approach is the doping with transition metals (such as chromium, iron, nickel, vanadium…). Nevertheless, these doped materials suffer of thermal instability and carrier recombination centres augmentation [5-12]. On the other hand, we have shown that the nitrogen

---

[*] Corresponding author: carmen.ristoscu@inflpr.ro

and carbon doping of TiO_2 thin films synthesized by pulsed laser deposition (PLD) significantly improved the photocatalytic activity under UV-vis irradiation [12]. As known, PLD allows for obtaining high purity thin films of single or multicomponent materials [13-15]. Incorporation of ZrO_2 in TiO_2 lattice was reported to enhance the specific surface area, the surface acidity and modify the photoelectrochemical properties leading to the improvement of the photocatalytic activity [16]. High resistance against aggressive media, regulation of the structure-sorption properties of the composites, stability to high-energy radiation and high anticorrosive properties of the photocatalytic coatings were gained by the mixing TiO_2 with ZrO_2 [17].

We report herewith on the PLD synthesis of TiO_2/ZrO_2 thin films doped with N_2. The photocatalytic activity of the obtained structures was tested for chromium toxic ions reduction.

2. Experimental

2.1. PLD

PLD experiments were carried out in a stainless steel irradiation chamber. Prior to any deposition, the chamber was evacuated down to a residual pressure of 10^{-4} Pa.

We used 50% ZrO_2 – 50%TiO_2 wt composite targets. The targets were ablated by a KrF* laser source (λ= 248 nm, τ_{FWHM} = 25 ns, υ=10 Hz). The laser beam was directed at 45^o on target surface by a 30 cm AR coated MgF_2 lens placed outside the irradiation chamber. The incident laser fluence was set at 1.6 J/cm^2. Series of 20,000 subsequent laser pulses were applied for the deposition of each film. During the multipulse laser ablation the targets were rotated with a frequency of 0.3 Hz and translated along 2 orthogonal axes to avoid drilling and ensure a uniform deposition, free of particulates.

Previous to introduction inside the deposition enclosure, the microscope glass substrates were successively cleaned in an ultrasonic bath in acetone, ethanol and deionized water for 15 min. The substrates were heated up to 600 ^{0}C during deposition and placed at 5 cm from target. The deposition area was 10x10 mm^2.

The depositions were performed in a low flux of high purity N_2, O_2, CH_4 or mixtures of 5:1 N_2/CH_4, 10:1 N_2/CH_4 or 1:1 N_2/O_2. The gas flux was monitored with MKS 100 controllers and the ambient pressure was stabilized to a constant value within the 3-10 Pa range. The data about the ambient gas nature and pressure during deposition together with the inferred values of the bandgap for all prepared samples were collected in Table I. In order to provide a statistically meaningful data set, we have prepared a series of five identical samples for each deposition condition.

Table I. Samples labeling, deposition gas nature and pressure, band gap energy and thickness of deposited films

Sample Code	***Target***	***Deposition ambiance***	***Pressure (Pa)***	$E_{g\ direct}$, ***eV***	***Thickness nm***
TZ1	TiO_2+ZrO_2	1:1 N_2/O_2	5	3.45	712
TZ2	TiO_2+ZrO_2	O_2	10	3.66	732
TZ3	TiO_2+ZrO_2	N_2	10	2.96	702
TZ4	TiO_2+ZrO_2	CH_4	10	3.23	648
TZ5	TiO_2+ZrO_2	10:1 N_2/CH_4	3	-	676
TZ6	TiO_2+ZrO_2	CH_4	5	-	684
TZ7	TiO_2+ZrO_2	5:1 N_2/CH_4	10	3.63	692

2.2. UV-Vis spectrophotometry

Optical spectra of the films were measured with a double beam spectrophotometer (Lambda 35, PerkinElmer) in the wavelength range of 190–1200 nm. To evaluate the band gap energy, the spectral dependences of the absorption coefficient (α) from $\alpha = 4\pi k/\lambda$ were obtained. The square and the square root of the absorption coefficient were plotted vs the light energy in the case of a direct and indirect semiconductor, respectively. In our case, the use of the square root is necessary to obtain the required linear relationship pointing on a direct electronic transition. The absolute error of band gap calculations was estimated as ± 0.02.

2.3. XRD

The XRD spectra of deposited structures were acquired with a Rigaku Ultima IV diffractometer equipped with multilayer structure (Cross Beam Optics) and with high precision vertical goniometer (θ-θ) of 285 mm radius. For phase analysis, the spectra were acquired in parallel beam setup, CuK_{α} radiation at grazing incidence ($\alpha = 1^0$) using the multi-purpose attachment (MPA) for thin films. Working conditions were set as anodic voltage $U_a = 4$ kV, anodic current $I_a = 30$mA, $2\theta \in (15^0, 85^0)$ or lower depending on sample, $\Delta(2\theta)=0.05^0$ and acquisition time per step $\tau = 2$s.

2.4. XPS

XPS spectra were explored with an electron spectrometer with PHOIBOS-100_SPECS energy analyzer. Nonmonochromatic MgK_{α} X-rays (1253.6 eV) were employed at P = 200 W. All the peaks of XPS spectra were charge corrected using C 1speak position as the reference point. Surface charge of the tested samples was in the range of 1.5-2.7 eV. Charge neutralization was performed using flood gun FG15/40 SPECS and aluminium screen-trap onto the sample**.** The vacuum in the working chamber was $2x10^{-7}$ Pa.

Spectra of Ti2p- та Zr3d- levels were deconvoluted onto connected with each other pairs of the components with consideration their spin-orbit splitting and parameters (Ti2p: $\Delta E = 5.76$ eB; $I_{1/2}/I_{3/2} = 0.5$, FWHM = 1.28 eB; Zr3d: $\Delta E = 2.4$ eB; $I_{3/2}/I_{5/2} = 0.66$, FWHM = 1.3 eB) Spectra of O1s- та N1s- levels were deconvoluted on the components with FWHM = 1.4 eB. The XPS signals were fitted using Gaussian-Newton method in the mode of bounded parameters. Variation of component intensity and bond energy was performed. Width of the components and ratio contribution of Gaussian-Lorentzian distribution for certain atoms of the tested samples in the process of spectrum deconvolution were fixed. The component square was determined after background subtraction by Shirley method. [18].

2.5. Photocatalytic activity

Photocatalytic activity of the films was assessed via Cr(VI) ions reduction reaction. The film was immersed in 40 ml of an aqueous solution of potassium bichromate (in all experiments, the initial concentration of bichromate ions was $2*10^{-4}$ M) and the reducing agent (disodium salt of ethylenediaminetetraacetic acid (Na_2EDTA)) in the molar ratio 1:1 adjusted to pH≥2 by perchloric acid. The reaction temperature was kept constant (25ºC) during the experimental procedure. The change of Cr(VI) ions concentration was monitored with a Lambda 35 UV-vis spectrophotometer (PerkinElmer) every 20 min. The reaction rate was attributed to pseudo-first order and inferred from the absorption intensity at λ=350 nm. The film was immersed in the solution until complete adsorption in the dark occurred, and then irradiated by 1000 W middle- pressure mercury lamp for 120 min. The distance lamp - reactor was set at 90 cm. Two blank experiments were carried out: the catalytic reduction of dichromate ions (dark condition), and photoreduction reaction (a bare glass was used instead of film). No significant changes in the absorption spectra of the liquid were observed for both blanks. For testing the visible light sensitivity, a filter transmitting light with $\lambda >$ 380 nm was introduced in the photocatalytic setup.

3. Results and discussion

The film thickness was measured by profilometry and found to be in the range 648 – 732 nm (Table I).

3.1. UV-Vis spectrophotometry

TiO_2/ZrO_2 films prepared in ambient N_2 and/or CH_4 atmospheres exhibited a different extension degree in the visible light absorption spectra. As visible from Fig. 1, the absorption onset at 340 nm for undoped TiO_2/ZrO_2 film deposited in 10 Pa O_2 (curve 3) coincides with that of pure TiO_2 film (curve 2) (synthesized on glass substrate heated at 600 °C from a TiO_2 target in 20 Pa oxygen). The pure ZrO_2 film (curve 1 in Fig. 1) was obtained from a ZrO_2 target in 20 Pa oxygen on glass substrates kept during deposition at 600 °C. A red shift up to 385 and 460 nm was observed for the TiO_2/ZrO_2 films deposited in ambient 1:1 N_2/O_2 (curve 4) and N_2 (curve 6), respectively.

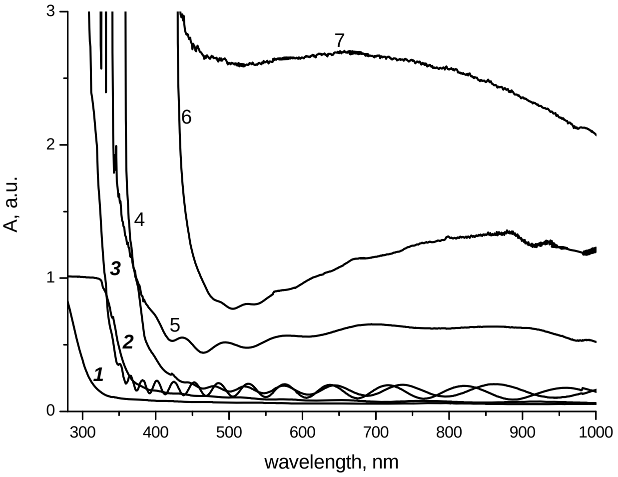

Fig. 1. Absorption spectra of ZrO_2 (1), TiO_2 (2), TZ2 (3), TZ1 (4), TZ7 (5), TZ3 (6), and TZ4 (7) films

According to our observations, the absorption in the visible region increases with the N_2 content in the ambient gas mixtures (compare curves 4, 5 and 6 in Fig. 1). A broad absorption in the visible region was noticed for the film deposited in CH_4 (curve 7, Fig 1). The narrowing of the band gap energy without any shift of the conduction and valence bands position is considered an effect of N - generated mid-gap level [19].

The influence of the doping agent nature and content was observed in the varied band-gap energy values (Table I). These values, E_g, were calculated by extrapolating the linear parts of the $(\alpha h\nu)^2 \sim f(h\nu)$ curves, i.e. assuming the direct electronic transition. On the other hand, for the doped composite samples TZ5 and TZ6, the calculation of E_g was impossible because of the strong absorption in the visible region.

3.2. XRD

All films were amorphous as confirmed by the recorded XRD patterns (Fig. 2). The amorphism could be explained by the existence of very small TiO_2 particles or by the presence of ZrO_2 in excess inhibiting the TiO_2 crystallization [20, 21]. Some incipient crystallization corresponding to the (101) line of ZrO_2 was observed for all samples. We cannot rule out the possible formation of some TiO_2 nanoparticles undetectable by XRD. Indeed, as mentioned in previous section, the onset of the absorption spectra of TiO_2/ZrO_2 and the TiO_2 films coincides (compare curves 2 and 4 in Fig. 1), while the binding energies of the Ti2p levels in both TiO_2/ZrO_2 and TiO_2 anatase are overlapping [12]. The crystallization of metal oxide was therefore not observed in bulk, but the anatase phase could appear on the surface (1-2 nm in depth).

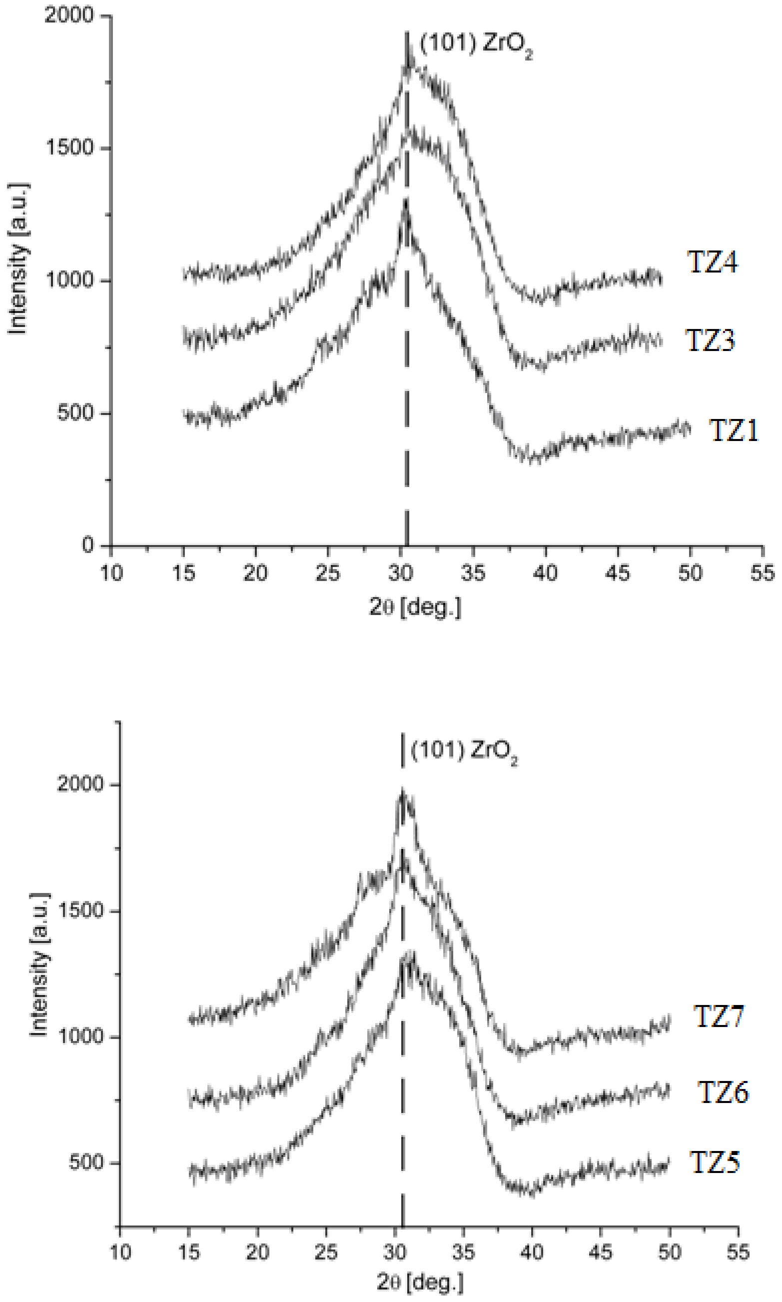

Fig. 2. XRD spectra of deposited TiO_2/ZrO_2 *thin films*

3.3. XPS

To investigate the surface structure and understand the origin of possible differences in the photocatalytic activity of samples, the films synthesized in pure N_2 (TZ3), CH_4 (TZ6) and their mixtures (TZ7 and TZ5) have been submitted to XPS investigations.

As shown the Ti 2p line of the sample synthesized in pure methane (Fig. 3A, b) contains two nonequivalent states. The dominating contribution in Ti2$p_{3/2}$ XPS spectra assigned to E_b = 458.8 eV (Fig. 3A, peak 3) corresponded to Ti^{4+} species in TiO_2. The Ti 2$p_{3/2}$ peak at 458.3 eV is also assigned to Ti^{4+} (Fig. 3A, peak 2), the decrease of E_b value indicates on the increase of Ti-O bond length. These peaks were also characteristic to undoped anatase film obtained in our laboratory by PLD method [12].

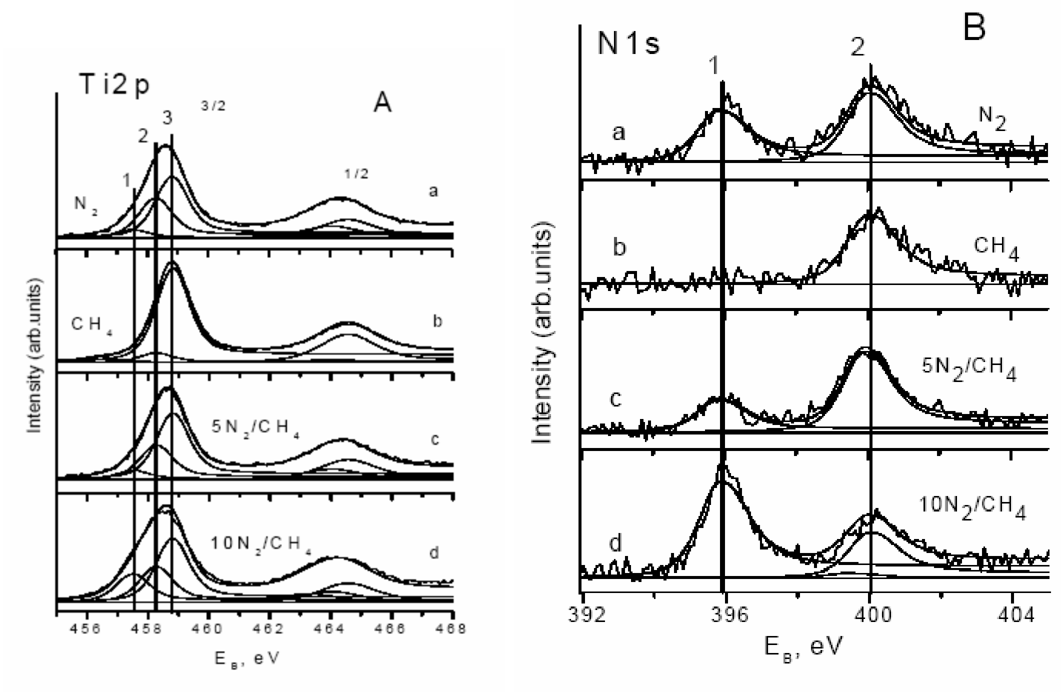

Fig. 3. XPS spectra of Ti2p (A) and N1s (B) energy for the samples TZ3 (a), TZ6 (b), TZ7 (c), TZ5 (d).

The peak 1 in Fig. 3A (E_b=457.5 eV) appeared in the spectra of the films obtained in N_2 and its mixtures with CH_4 could be assigned to the O-Ti-N bonds, as mentioned in Refs. 22-24. Appearance of deconvoluted peak at this range of E_b values in Ti 2p line was also sign to the formation of titanium Ti^{3+} species suggesting the existence of oxygen vacancies [25]. In our previous study the Ti2p peak at 457.5 eV was not registered for undoped titania film [12]. In addition to this, N1s spectra of the films synthesized only in N_2 contained gas mixtures indicate the nitrogen atom incorporation in titania. Thus, we suggest that the peak at 457.5 eV belongs to the Ti-N bond rather than oxygen vacancies. It must be emphasized that spectra of the TZ.5 sample contains the most contribution of the peaks such as Ti2$p_{3/2}$ at E_b= 457.5 eV and N1s with E_b = 395.8 eV (tables II) indicating more nitrogen incorporation in the bonds. The comparison of XPS data of TZ3, TZ5 and TZ7 samples points out to the existence of an optimum content of methane in the process of the N-doped semiconductor films synthesis by PLD method. It is suggested that the carbon from N_2/CH_4 mixture interacts with oxygen from TiO_2 leading to the formation of an oxygen deficient lattice and, in turn, assists an efficient embedding of nitrogen atom. This could result in the higher efficiency of O-Ti-N as compared to O-Ti-O fragments formation.

The binding energy of Zr3$d_{5/2}$ peak for all samples (not shown here) is 182.3 eV corresponding to Zr^{4+} states in ZrO_2 [26]. This correlates with the results reported herein [27] where only the peak with E_B Zr3$d_{5/2}$= 182.3 eV was observed at high content of zirconium in titania matrix. ..

The peak 1 with 395.9 eV is pointing to the Ti-N bond formation by the atomic substitution of oxygen with nitrogen [28, 29] as shown on N1s spectra (Fig. 3B). The peak 2 of nitrogen (400.0 eV) (Fig. 3B) was assigned [29, 30] to the nitrogen adsorption from air in the film. The spectrum of the sample TZ6 deposited in methane also contains interstitial nitrogen resulting from N_2 adsorption in the forming structure. It follows that N-doping does not occur in the gas phase, but rather in the film structure after heating [31]. Almost equal intensity of the peaks at 395.8 and 400.0 eV was observed for the sample TZ3 deposited in pure N_2. More Ti-N bonds were noticed in case of sample TZ5 as the intensity of the peak at 395.9 eV was raising (Table II). As in the case of Ti 2p spectra, this indicates that carbon species forming as a result of laser action react with oxygen one causing the subsequent oxygen substitution by nitrogen atoms. This mechanism is supported by the XPS evidence according to which the intensity of peak at 395.9 eV was lower in case of samples TZ3 vs. TZ5, even though the synthesis was conducted in the first case in a pure N_2 atmosphere

Table II. XPS relative intensities of Ti2p$_{3/2}$ - N1s- and O1s- peaks

$E_{b,}$/Sample	TZ3	TZ5	TZ6	TZ7
	I, (%)	I, (%)	I, (%)	I, (%)
Ti2p$_{3/2}$ 457.5 eV	7.5	23.5	-	8.1
Ti2p$_{3/2}$ 458.3 eV	36.9	27.8	9.0	31.7
Ti2p$_{3/2}$ 458.8 eV	55.6	48.7	91.0	60.2
N 1s 395.8 eV	42.5	67.6	-	28.7
N 1s 400.0 eV	57.5	32.4	100	71.3
O 1s 530.1 eV	66.5	67.4	89.9	58.9
O 1s 531.7 eV	17.4	12. 9	-	17.7
O 1s 532.5 eV	11.0	15.5	10.1	15.0
O 1s 533.2 eV	5.1	4.2	-	8.4

The peak of O1s spectra with E_b=530.1 eV (Table II) is assigned to O^{2-} species of titanium-oxygen and zirconium-oxygen bonds. The binding energy at 531.7 eV is attributed to the lower electron density oxygen species as “O^-” compensating for deficiencies at the TiO_2 surface [26] or the presence of OH groups. The peaks at E_b=532.5 eV and E_b=533.2 eV are connected with OH-groups and H_2O, respectively. The lowest content of O^-, OH^-species and H_2O for sample TZ6 is indicative for a less defective surface in comparison with the other films.

Miyauchi *et al.* [32] synthesized carbon-doped titania by oxidizing TiC and observed the C1s peak at a much lower binding energy (281.8 eV). They assigned this peak to the Ti–C bond in carbon-doped anatase phase. The other two features at 288.1 and 286.3 eV were attributed to C–N and C–O bonds, respectively. In our case, the elementary carbon peaking at 285 eV [33] and a small fraction of oxidized carbon (286.4 eV) [30] were observed (not shown here) by scanning the C1s region. We assumed that no Ti-C bonds were present in the structure of the films. It must be emphasized that the C1s signal was not detected for the film obtained in pure nitrogen (TZ3).

Overall, the presence of nitrogen as well as its mixture with methane in the synthesis chamber leads to the appearance of Ti2p$_{3/2}$ state with E_b=457.5 eV and N 1s state with E_b=395.8 eV, (table II) reflecting the formation of O-Ti-N bonds in the oxide matrix. The TZ5 film synthesized at minimum methane content in N_2/CH_4 mixture and minimum pressure exhibits the maximum reaction rate constant of photodegradation as well as the highest possible distribution of Ti2p and N1s states connected to O-Ti-N bonds. Interaction of formed under laser pulse carbon atoms and radicals with oxygen atoms of O-Ti-O fragments leads to the formation of oxygen vacancies and increase of O-Ti-N fragments is suggested. Stronger Zr-O bond is invariably remained at this condition.

3.4. Photocatalytic activity

The photocatalytic activity of doped films was monitored in the process of the toxic Cr(VI) ions photoreduction to non-toxic Cr(III) ions in aqueous media by exposure to visible or UV light. The films were inert under visible light irradiation showing an activity similar to that of blank sample. Bare zirconium oxide film possessed much lower activity comparing to bare TiO_2 film under UV light. An improvement of the photocatalytic performance compared to TiO_2 film was observed under UV light exposure of TiO_2/ZrO_2 film containing double doping agent (TZ5). The highest reaction rate constant (Table III) was reached for the structure with the largest number of O-Ti-N bonds. We suggest that the O-Ti-N bonds (E_b = 395.8 eV) improve the electron-hole separation, while the interstitial N atoms (E_b = 400.0 eV) incorporated in semiconductor structure are inert as the electron/hole traps in photoreduction under UV and Vis - light irradiation.

Table III. The reaction rate constant of studied samples for Cr^{6+} to Cr^{3+} photoreduction under full light irradiation

Sample	K, sec^{-1}
TZ1	$3.1*10^{-5}$
TZ2	$3.0*10^{-5}$
TZ3	$3,5*10^{-5}$
TZ4	$3,5*10^{-5}$
TZ5	**$8,4*10^{-5}$**
TZ6	$2,2*10^{-5}$
TZ7	$2,5*10^{-5}$
TiO_2	$7,0*10^{-5}$
ZrO_2	$2,2*10^{-5}$

Thus, the TiO_2 band-gap narrowing is mandatory for extending the photocatalytic action to visible light. Nevertheless, other factors such as an effective trapping of photogenerated charge carriers, adsorption/desorption of reaction components and appropriate redox couples could crucially influence the recombination rate of an electron-hole pair. Even though Ti-C bonds have not been detected on the surface, we suppose that the improvement of photocatalytic activity of nitrogen-containing films is connected with promoting action of carbon in the incorporation of nitrogen atoms into the semiconductor structure (TZ5). It is suggested that the defects in TiO_2/ZrO_2 matrix caused by chemical bonding of N and Ti atoms act as traps for the electron/hole.

4. Conclusions

The influence of synthesis conditions on the efficiency of nitrogen incorporation in the presence of double doping agents (N_2/CH_4) was studied. The presence of low content of CH_4 in deposition ambiance (10:1 N_2/CH_4) assisted the formation of O-Ti-N fragments in metal oxide matrix as evidenced from the remarkable appearance of $Ti2p_{3/2}$ (E_b=457.5 eV) and N1s (E_b=395.8 eV) peaks in XPS spectra. It followed that the nitrogen incorporation induced the traps for charges photogenerated by light leading to the improvement in photocatalytic reduction of toxic Cr(VI) to Cr(III) under UV light.

Acknowledgements

OL, IP, NS, AE, GS, NS, CR and INM acknowledge with thanks the support of this work under the exchange program “Physical and chemical approaches to the synthesis of visible-light sensitive semiconductor films for photo-catalytic application” between Academy of Sciences of Ukraine and Romanian Academy. GS, NS, CR and INM acknowledge with thanks the support of

UEFISCDI under the contract ID 304/2011. VDj and DjJ wish to acknowledge the financial support from Ministry of Science and Technological Development of the Republic of Serbia through the project III 45019.

References

[1] K. Hashimoto, H. Irie, A. Fujishima, TiO_2 Photocatalysis: A Historical Overview and Future Prospects, Jpn. J. Appl. Phys. **44** 8269-8285 (2005)

[2] M. Anpo, Preparation, Characterization, and Reactivities of Highly Functional Titanium Oxide-Based Photocatalysts Able to Operate under UV–Visible Light Irradiation: Approaches in Realizing High Efficiency in the Use of Visible Light, Bull. Chem. Soc. Jpn. **77,** 1427-1442 (2004)

[3] A. Kudo, H. Kato, I. Tsuji, Strategies for the Development of Visible-light-driven Photocatalysts for Water Splitting, Chem. Lett. **33** 1534-1539 (2004)

[4] T.L. Thompson, J.T. Yates Jr., Surface Science Studies of the Photoactivation of TiO_2 New Photochemical Processes, Chem. Rev. **106** 4428-4453 (2006)

[5] A.K. Ghosh, H.P. Maruska, Photoelectrolysis of Water in Sunlight with Sensitized Semiconductor Electrodes, J. Electrochem. Soc. **124** 1516-1522 (1977)

[6] W. Choi, A. Termin, M.R. Hoffmann, The Role of Metal Ion Dopants in Quantum-Sized TiO2: Correlation between Photoreactivity and Charge Carrier Recombination Dynamics, J. Phys. Chem. **98** 13669–13679 (1994)

[7] A.L. Linsebigler, G.Q. Lu, J.T. Yates, Photocatalysis on TiO_2 Surfaces: Principles, Mechanisms, and Selected Results, Chem. Rev. **95** 735-758 (1995)

[8] H. Irie, Y. Watanabe, K. Hashimoto, Nitrogen-Concentration Dependence on Photocatalytic Activity of $TiO_{2-x}N_x$ Powders, J. Phys. Chem. B **107** 5483-5486 (2003)

[9] T. Morikawa, R. Asahi, T. Ohwaki, K. Aoki, Y. Taga, Band-Gap Narrowing of Titanium Dioxide by Nitrogen Doping, Jpn. J. Appl. Phys. **40** L561-L563 (2001)

[10] S. Sakthivel, H. Kisch, Photocatalytic and Photoelectrochemical Properties of Nitrogen-Doped Titanium Dioxide, Chem. Phys. Chem. **4** 487-490 (2003)

[11] T. Ohno, M. Akiyoshi, T. Umebayashi, K. Asai, T. Mitsui, M. Matsumura, Preparation of S-doped TiO_2 photocatalysts and their photocatalytic activities under visible light, Appl. Catal. A-Gen. **265** 115-121 (2004)

[12] G. Socol, Yu. Gnatyuk, N. Stefan, N. Smirnova, C. Sutan, V. Malinovski, A. Stanculescu, O. Korduban, I. N. Mihailescu, Photocatalytic activity of pulsed laser deposited TiO_2 thin films in N_2, O_2 and CH_4, Thin Solid Films **518** 4648-4653 (2010)

[13] E. Gyorgy, G. Socol, E. Axente, I. N. Mihailescu, C. Ducu, S. Ciuca, Anatase phase TiO_2 thin films obtained by pulsed laser deposition for gas sensing applications, Appl. Surf. Sci. **247** 429-433 (2005)

[14] D. Caiteanu, E. Gyorgy, S. Grigorescu, I. N. Mihailescu, G. Prodan, V. Ciupina, Growth of oxide thin films for optical gas sensor applications, Appl. Surf. Sci. **252** 4582-4586 (2006)

[15] Ion N. Mihailescu, Carmen Ristoscu, Adriana Bigi, Isaac Mayer, Advanced biomimetic implants based on nanostructured coatings synthesized by pulsed laser technologies, Chapter 10 in "Laser-Surface Interactions for New Materials Production Tailoring Structure and Properties", Series: Springer Series in Materials Science, Vol. 130, Miotello, Antonio; Ossi, Paolo M. (Eds.), pp. 235 – 260 (2010)

[16] Yu. Gnatyuk, N. Smirnova, A. Eremenko, V. Ilyinl, Design and Photocatalytic Activity of Mesoporous TiO_2/ZrO_2 Thin Films, Adsorption Science & Technology **23** 497-508 (2005)

[17] N.V Vituk, N.P. Smirnova, A.M. Eremenko, I.P. Bukov, Influence of high-energy irradiation on formation of defects in individual and mixed oxide SiO_2-TiO_2-ZrO_2, Surface **2** ISBN 978-966-00-0834-1, 161-171 (2010)

[18] D. Briggs, M.P. Seach, Practical surface analysis by Auger and X-ray photoelectron spectroscopy, John Wiley & Sons, Chichester - New York (1983)

[19] Y. Wang, D.J. Doren, First-principles calculations on TiO_2 doped by N, Nd, and vacancy, Solid State Commun. **136** 186-189 (2005)

[20] M.E. Manrıquez, T. Lopez, R. Gomez, J. Navarrete, Preparation of TiO_2–ZrO_2 mixed oxides

with controlled acid–basic properties, J. Molec. Catal. A: Chemical. **220** 229–237 (2004)

[21] Y. Wan, J. Ma, W. Zhou, Y. Zhu, X. Song, H. Li. Preparation of titania-zirconia composite aerogel materials by sol-gel combined supercritical fluid drying, Appl. Catal. **277** 55-59 (2004)

[22] Y. Nakano, T. Morikawa, T. Ohwaki, Y. Taga, Origin of visible-light sensitivity in N-doped TiO_2 films, Chem. Phys. **339** 20-26 (2007)

[23] C. di Valentin, E. Finazzi, G. Pacchioni, A. Selloni, S. Livraghi, M. C. Paganini, E. Giamello, N-doped TiO_2: Theory and experiment, Chem. Phys. **339** 44-56 (2007)

[24] S.A. Chambers, S.H. Cheung, V. Shutthanandan, S. Thevuthasan, M.K. Bowman, A.G. Joly, Properties of structurally excellent N-doped TiO_2 rutile, Chem. Phys. **339** 27-35 (2007)

[25] Abdul K. Rumaiz, BakhtyarAli, Abdullah Ceylan, M. Boggs, T. Beebe, S. Ismat Shah, Experimental studies on vacancy induced ferromagnetism in undopedTiO_2, Solid State Communications **144** 334-338 (2007)

[26] J.C. Dupin, D. Gonbeau, P. Vinatier, A. Levasseur, Systematic XPS studies of metal oxide, hydroxides and peroxides, Phys.Chem.Chem.Phys. **2** 1319-1324 (2000)

[27] Yu. Gnatuk, N. Smirnova, O. Korduban, A. Eremenko, Effect of zirconium incorporation on the stabilization of TiO_2 mesoporous structure, Surface and Interface Analysis **42** 1276-1280 (2010)

[28] N.C. Saha, H.G. Tompkins, Titanium nitride oxidation chemistry. An X-ray photoelectron spectroscopy study, J. Appl. Phys. **72** 3072-3079 (1992)

[29] J. Yang, H. Bai, Q. Jiang, J. Lian, Visible-light photocatalysis in nitrogen–carbon-doped TiO_2 films obtained by heating TiO_2 gel–film in an ionized N_2 gas, Thin Solid Films **516** 1736-1742 (2008)

[30] J. Yang, H. Bai, X. Tan, J. Lian, IR and XPS investigation of visible-light photocatalysis—Nitrogen–carbon-doped TiO_2 film, Appl. Surf. Sci. **253** 1988-1994 (2006)

[31] S. Somekawa, Y. Kusumoto, M. Ikeda, B. Ahmmad, Yu. Horie, Fabrication of N-doped TiO_2 thin films by laser ablation method: Mechanism of N-doping and evaluation of the thin films, Catalysis Communications **9** 437-440 (2008)

[32] M. Miyauchi, A. Ikezawa, K. Hashimoto, Zeta potential and photocatalytic activity of nitrogen doped TiO_2 thin films, Phys. Chem. Chem. Phys. **6** 865-870 (2004)

[33] L. Mai, C. Huang, D. Wanga, Z. Zhang , Y. Wang, Effect of C doping on the structural and optical properties of sol–gel TiO_2 thin films, Appl. Surf. Sci. **255** 9285-9289 (2009)